

## 141. Transfer Mechanism of Ionic Drugs: Piroxicam as an Agent Facilitating Proton Transfer

by Frédéric Reymond<sup>a</sup>), Guillaume Steyaert<sup>b</sup>), Alessandra Pagliara<sup>b</sup>), Pierre-Alain Carrupt<sup>b</sup>), Bernard Testa<sup>b</sup>), and Hubert Girault<sup>a</sup>)\*

<sup>a</sup>) Laboratoire d'Electrochimie, Ecole Polytechnique Fédérale de Lausanne, CH-1015 Lausanne

<sup>b</sup>) Institut de Chimie Thérapeutique, Section de Pharmacie, Université de Lausanne, CH-1015 Lausanne

(6. VI. 96)

---

Facilitated proton transfer may be of potential significance in pharmacokinetic and pharmacodynamic processes. Here, we show that the NSAID piroxicam and its *N*- and *O*-methylated derivatives act as ionophores for proton transfer across the H<sub>2</sub>O/1,2-dichloroethane interface. Investigations by cyclic voltammetry showed that the proton transfer occurs by interfacial protonation of the ionophore. The dissociation constants of the three compounds in the organic phase were calculated by *Matsuda*'s theory. With this particular transfer mechanism, the present study exemplifies how electrochemistry at a liquid/liquid interface can be applied to calculate the fundamental thermodynamic parameters related to the pharmacokinetic behavior of ionic drugs.

---

**1. Introduction.** – The pharmacokinetics of drugs and other xenobiotics in the body is determined mainly by their interactions with biological membranes. While drug-receptor interactions have received most of the attention in drug design, the mechanistic implications of membrane permeation has been largely underestimated. Due to the complex structure of membranes [1] [2], the mechanisms of their interactions with bioactive compounds may be as intricate as those governing ligand-receptor interactions [3]. Beside passive diffusion controlled mainly by lipophilicity [4], the existence of more complex mechanisms is now recognized. In particular, the membrane partitioning of ionized species has been documented [5–10].

Proton activity (*i.e.*, pH) is one of the most tightly regulated physicochemical parameters in functional biological systems. At the level of organisms, the pH is controlled mainly by buffer systems (*e.g.* 0.6 mM albumin and 20 mM carbonate in human serum), by active renal secretion of protons and other ions (*e.g.* carbonate and phosphate), by dermal excretion of various acids, and by pulmonary elimination of CO<sub>2</sub>. At the level of cells and sub-cellular organelles, active transport systems act to import or export protons. For example, the Na<sup>+</sup>/H<sup>+</sup> antiport plays great role in the normal function of neutrophils [11]. Similarly, complexes I–IV of the mitochondrial electron transport generate a proton gradient which is used by complex V to produce ATP [12].

A large number of pathological or unwanted states involve dysregulation of pH levels in organelles, cells, and tissues. Oxidative stress to which mitochondria are particularly sensitive is one example [12]. Multidrug resistance is a complex phenomenon in which alkalization of the cytosol also plays a role [13]. Perhaps the most studied example is that of inflammation and rheumatism which decrease pH in extracellular media such as the synovial fluid [14].

In recent years, much research has been devoted toward agents able to alter pH levels, more precisely to correct for dysregulations. Examples are compounds that act on the  $\text{Na}^+/\text{H}^+$  antiport or on lysosomes [13] [15] [16]. A number of modern anti-inflammatory drugs or drug candidates are being found to influence pH levels as a synergistic mechanism to their principal activity as inhibitors of cyclooxygenase and radical scavengers. One recently uncovered mechanism involves entry of some drugs as the conjugate acid into the cellular compartment; there, the drug dissociates, and the anion is actively exported from the cell, the net result being an alkalization of extracellular fluids [17].

In analogy with ion-transfer reactions facilitated by ionophores [18–24], proton transfer mediated by either electroneutral [25–30] or ionized ionophores [31–34] has been reported in the literature. These studies show that both the pH of the aqueous phase and ionophore concentration in the organic phase influence the nature and type of the facilitated ion-transfer reaction. When the proton is the species liable to transfer, two general charge-transfer mechanisms have been proposed [35]. In ‘direct’ transfer, the ligand is protonated in the bulk aqueous phase and may subsequently transfer, if a suitable electrical potential is applied between the two phases. In ‘facilitated’ transfer the ionophore forms a complex with the proton at the interface and allows transfer to proceed by either interfacial complexation (transfer by interfacial complexation: TIC) or interfacial dissociation (transfer by interfacial dissociation: TID) depending on the phase in which the ligand is present initially.

The present paper deals with the transfer mechanisms of piroxicam and two inactive derivatives (*N*-Me- and *O*-Me-piroxicam) at the  $\text{H}_2\text{O}/1,2$ -dichloroethane ( $\text{ClCH}_2\text{CH}_2\text{Cl}$ ) interface. Cyclic voltammetry at the interface between two immiscible electrolyte solutions (ITIES) was used to determine the nature of the transfer and to show the influence of the ionic forms of the piroxicams on the transfer. *Matsuda*'s methodology [36] was then employed to interpret the aqueous pH dependence of the transferring species and to evaluate the dissociation constants of the piroxicams in the organic phase.

**2. Experimental.** – Bis(triphenylphosphoranylidene)ammonium tetrakis(4-chlorophenyl)borate ( $[(\text{Ph}_3\text{P})_2\text{N}]^+[\text{B}(\text{ClC}_6\text{H}_4)_4]^-$ ) was prepared by metathesis of  $\text{K}[\text{B}(\text{ClC}_6\text{H}_4)_4]$  (*Lancaster*, UK) and of bis(triphenylphosphoranylidene)ammonium chloride ( $(\text{Ph}_3\text{P})_2\text{NCl}$ ; *Fluka*, CH) and recrystallized twice from MeOH. The org.-phase solvent was 1,2-dichloroethane ( $\text{ClCH}_2\text{CH}_2\text{Cl}$ ) (*AnalaR*, *Merck*, D) and was used without further purification. All necessary precautions were taken in the handling of  $\text{ClCH}_2\text{CH}_2\text{Cl}$  [37]. Piroxicam (= 4-hydroxy-2-methyl-*N*-(pyridin-2-yl)-2*H*-1,2-benzothiazine-3-carboxamide 1,1-dioxide) was supplied by *Sigma* (CH) and used without further purification. *N*-Me-piroxicam (= 4-hydroxy-2-methyl-*N*-(1-methylpyridin-2-yl)-2*H*-1,2-benzothiazine-3-carboxamide 1,1-dioxide) and *O*-Me-piroxicam (= 4-methoxy-2-methyl-*N*-(pyridin-2-yl)-2*H*-1,2-benzothiazine-3-carboxamide 1,1-dioxide) were synthesized according to the method of *Hammen et al.* [38] [39].  $\text{HNO}_3$ , LiOH, anh. LiCl,  $\text{Li}_2\text{SO}_4$ , KCl, MeOH, and  $(\text{Me}_4\text{N})_2\text{SO}_4$  were all supplied by *Fluka*. All reagents used were of anal. grade or purer.

The electrochemical apparatus used was a four-electrode potentiostat (Southampton University, UK), of a design similar to that given in [40] with *iR* drop compensation. The scanning of the applied potential was performed by a waveform generator *PPRI* (*Hi-Tek Instruments*, UK), which was coupled to an *X-Y* recorder (*Bryans Instruments*, UK). The cell used was constructed of glass and was of the same design as used previously [40], with a surface area of  $1.13 \pm 0.02 \text{ cm}^2$ . Both the cell and the four-electrode potentiostat were housed in a *Faraday* cage, and the cell was kept at r.t. ( $21 \pm 2^\circ$ ) for all experiments. All the half-wave potentials were referred to the half-wave potential of  $\text{Me}_4\text{N}^+$  and obtained by adding a predetermined amount of  $(\text{Me}_4\text{N})_2\text{SO}_4$  to the cell for each experiment.

When used in the aq. phase, piroxicam and its derivatives were injected into an aq. LiCl soln. (base electrolyte) before filling the cell. As they dissolved only sparingly, the pH of the  $\text{H}_2\text{O}$  soln. was reduced between two and three units with conc.  $\text{HNO}_3$ . The pH was then adjusted to the desired value with  $\text{HNO}_3$  or LiOH, so as to form a 1 mM

piroxicam (or derivative) and 10 mM LiCl soln. This constituted the aq. phase, and the volume added to the cell in each experiment was always precisely 1.7 ml, so that a constant concentration of piroxicam was maintained throughout.

When used in  $\text{ClCH}_2\text{CH}_2\text{Cl}$ , the piroxicams were found to dissolve easily. The org. phase could then be formed without complication and the volume added to the cell was also precisely 1.7 ml, so as to minimize experimental errors on concentration.

In this paper, the transfer of a cation from the aq. to the  $\text{ClCH}_2\text{CH}_2\text{Cl}$  phase is defined as a positive current. This relates to the fact that the potential of  $\text{H}_2\text{O}$  with respect to the org. phase is made more positive on the forward scan, a convention valid for all experiments at the ITIES. Using this definition, the voltammogram of the cation which transfers with a lower applied potential needs less energy to cross the interface and thus represents a more hydrophobic species. On the reverse scan, the transfer of a cation from the  $\text{ClCH}_2\text{CH}_2\text{Cl}$  to the aq. phase generates a negative current.

The  $\text{ClCH}_2\text{CH}_2\text{Cl}/\text{H}_2\text{O}$  partition coefficients ( $\log P$ ) of the three compounds were measured by a two-phase titration method (*Sirius*) [41] or by centrifugal partition chromatography (CPC) [42] [43], and are given in *Table 1*. A solvatochromic analysis of  $\text{H}_2\text{O}/\text{ClCH}_2\text{CH}_2\text{Cl}$  partition coefficients [44] shows that they resemble closely  $\text{H}_2\text{O}/\text{alkane}$  partition coefficients in terms of the balance of hydrophobic and H-bonding forces. The acid-base equilibrium constants of piroxicams in the aq. phase were taken from [39] [45] [46] and are also summarized in *Table 1*.

Table 1.  $\text{ClCH}_2\text{CH}_2\text{Cl}/\text{H}_2\text{O}$  Partition Coefficients and Dissociation Constants in the Aqueous Phase for Piroxicam and Derivatives

	$\log P$	$\text{p}K_{\text{a}1}^{\text{w}}$	$\text{p}K_{\text{a}2}^{\text{w}}$
Piroxicam	$3.10 \pm 0.10^{\text{a}}$	$1.86 \pm 0.02$	$5.46 \pm 0.02$
<i>N</i> -Me-Piroxicam	$1.20 \pm 0.05^{\text{b}}$	$1.05 \pm 0.04$	–
<i>O</i> -Me-Piroxicam	$2.07 \pm 0.10^{\text{a}}$	$2.72 \pm 0.04$	–

<sup>a</sup>) Measured with the *PCA 101* two-phase titrator. <sup>b</sup>) Measured by CPC.

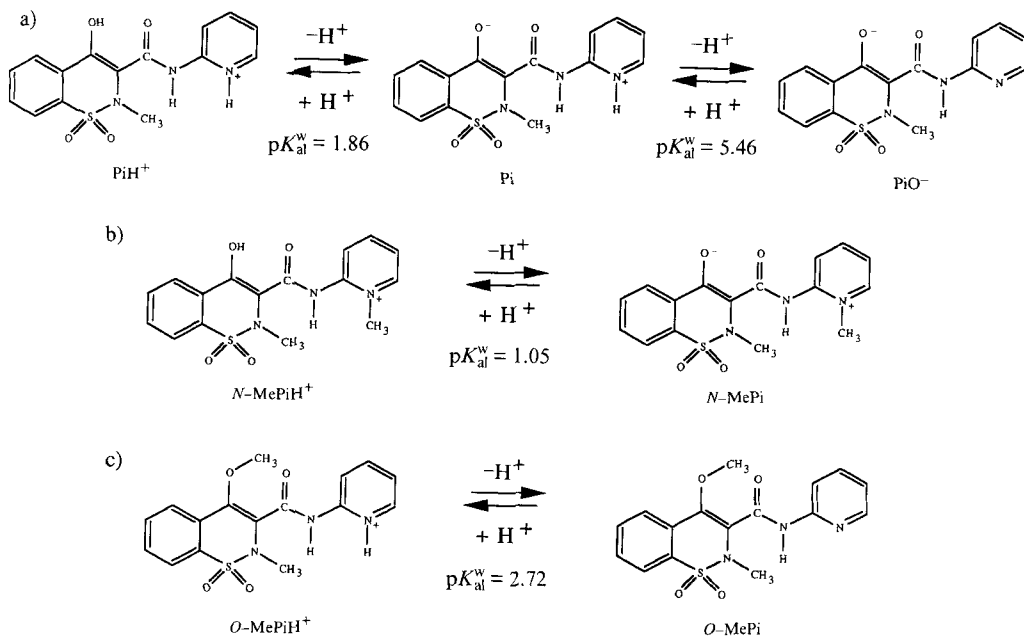
**3. Results and Discussion.** – 3.1. *Protonation Equilibria.* Piroxicam is of great pharmacological and therapeutic interest, being a long-lasting non-steroidal anti-inflammatory drug (NSAID) with limited gastric mucosal side effects, its dynamic structural features are also of particular chemical interest, because of its zwitterionic nature and its tautomeric structure [39] [46]. Two inactive derivatives of piroxicam are also used in this study, namely *N*-Me-piroxicam and *O*-Me-piroxicam (*Scheme*). The first compound cannot undergo protonation at the pyridyl function and the second cannot be ionized at the enolic group.

Piroxicam bears a weakly basic pyridyl group and an enolic function, resulting in a zwitterionic nature. The presence of the basic pyridyl function enhances the acidity of the enolic group and, consequently, influences its lipophilicity, as shown by determination of its physicochemical and structural properties [46] and by investigation of its microscopic protonation/deprotonation behavior [39]. Thus, these  $\text{p}K_{\text{a}}$  values allow a prediction on the nature of piroxicam and its derivatives, on their global charge, and on their transfer behavior at various pH values.

On the basis of the protonation equilibria described in the *Scheme*, it is possible to predict the expected structure and corresponding response at the liquid/liquid interface of the three compounds:

a) Piroxicam:

- Below pH 1.86: the pyridyl and enolic group are mostly protonated and the global charge is positive.

Scheme. Protonation Equilibria of a) Piroxicam, b) *N*-Me-Piroxicam, and c) *O*-Me-Piroxicam

- Between pH 1.86 and 5.46: the enolic function loses its proton, and piroxicam is mostly in zwitterionic form. As such, no transfer can be measured by cyclic voltammetry, since the global charge is zero.
- Above pH 5.46: the pyridyl group is mostly deprotonated and the global charge is then negative.

b) *N*-Me-piroxicam:

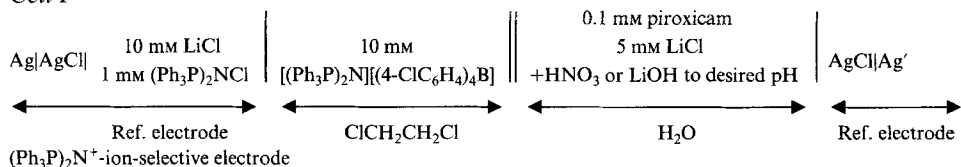
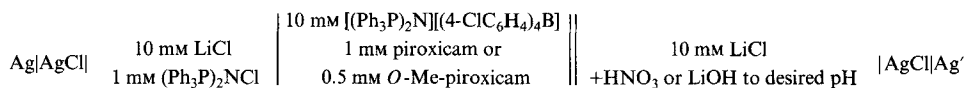
- Below pH 1.05: a positive charge remains on the pyridyl group, which can be detected by electrochemistry.
- Above pH 1.05: the enolic function loses a proton, resulting in a zwitterionic species which cannot be detected by cyclic voltammetry.

c) *O*-Me-piroxicam:

- Below pH 2.72: the pyridyl group is mostly positively charged and, under an applied potential, will cross the interface.
- Above pH 2.72: the pyridyl group is mostly not protonated, the molecule is in its neutral form and cannot be observed electrochemically.

3.2. *Formal Potential Dependence on pH.* Transfer studies of piroxicam and its derivatives were achieved using cyclic voltammetry at the ITIES. This technique allows the determination of the half-wave potential ( $\Delta_s^{\text{w}}\phi_i^{1/2}$ ) and the formal Gibbs energy of transfer ( $\Delta G_{\text{tr},i}^{0,\text{w}\rightarrow\text{o}}$ ) of the ionic forms.

Two different sets of experiments were performed with this methodology. First, piroxicam and its derivatives were dissolved in the aqueous phase at a predetermined concentration as described in *Cell I*. In the second series, they were dissolved in the organic phase, as shown in *Cell II*.

**Cell I**

**Cell II**


The experimental values of  $\Delta_o^w \phi_i^{1/2}$  were referenced for each measurement against the transfer of the  $\text{Me}_4\text{N}^+$  cation. It is then possible to calculate a value for the formal transfer potential of an ion  $i$  ( $\Delta_o^w \phi_i^0$ ) using the relationship in Eqn. 1, if we assume that Walden's rule ( $D^w D^o = \eta^w \eta^o$ ) applies for the transfer of ionic forms of  $\text{Me}_4\text{N}^+$ , piroxicam, and its derivatives.

$$\Delta_o^w \phi_{i(\text{exp})}^{1/2} - \Delta_o^w \phi_i^0 = \Delta_o^w \phi_{\text{Me}_4\text{N}^+(\text{exp})}^{1/2} - \Delta_o^w \phi_{\text{Me}_4\text{N}^+}^0 \quad (1)$$

On the tetraphenylarsonium tetraphenylborate ( $[\text{Ph}_4\text{As}][\text{Ph}_4\text{B}]$ ) scale, a value of 160 mV for  $\Delta_o^w \phi_{\text{Me}_4\text{N}^+}^0$  [47] was determined, it was used as a reference for the determination of the formal transfer potentials of the ions and, thus, for the calculation of their formal Gibbs transfer energy [48]:

$$\Delta_o^w \phi_i^0 = \frac{\Delta G_{\text{tr},i}^{0,w \rightarrow o}}{z_i F} \quad (2)$$

Cyclic voltammetry can demonstrate the dependence of the half-wave potential on aqueous pH and should allow the determination of the nature of the transferring species, since the ionic composition of the piroxicam solution depends on the proton concentration. Fig. 1 shows several voltammograms obtained at different pH values with Cell II.

This figure shows that only one peak appears at low pH, and, consequently, that only one species can cross the interface. The shape of the voltammograms indicates that transfer is reversible and, therefore, diffusion-controlled, implying very fast ion transport across the interfacial region.

Transfer is limited by diffusion as shown by the linear dependence of the maximum peak current on the square root of the sweep rate, according to the Randles-Sevcik equation [49]. The peak-to-peak separation is ca. 60 mV, which complies with the conditions for a reversible transfer of a singly charged ion (since the potential difference between the forward and the reverse peaks is given by the ratio:  $RT/zF = 59z$  [mV] [50]).

The half-wave-potential shifts toward higher potential values when the pH in the aqueous phase increases. When the pH is 5.88, the forward peak is obscured by the end of the potential window, and only the reverse peak is observable. Above pH 6, no peak current can be measured, because the half-wave potential of the transferring species lies outside the potential window.

The same behavior was observed with *O*-Me-piroxicam. The transfer wave disappears at almost the same pH value and the shift of potential is approximately the same as

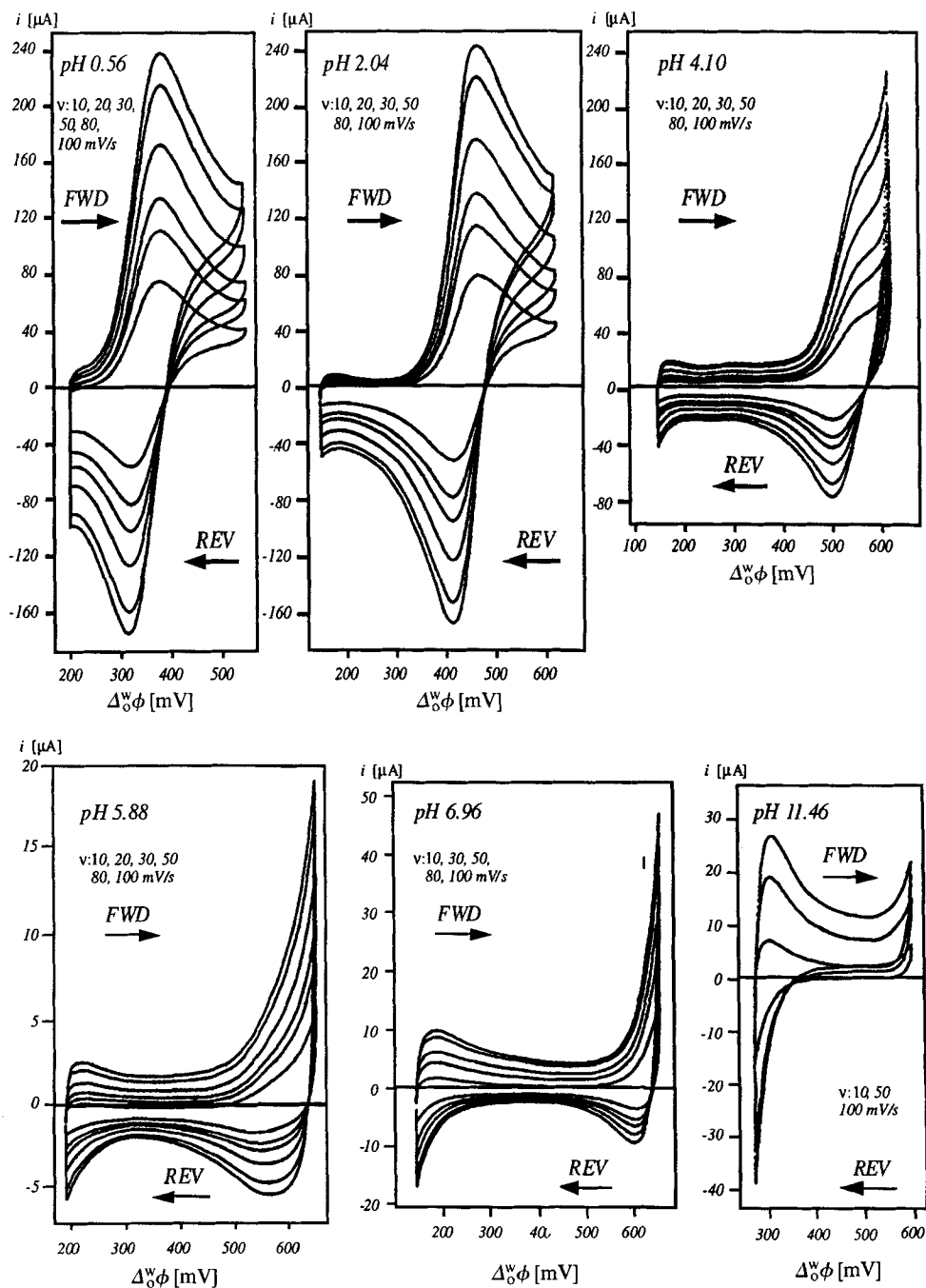


Fig. 1. Typical cyclic voltammograms at various pH values for piroxicam used in Cell II (FWD = forward scan; REV = reverse scan)

with piroxicam. Moreover, when piroxicam and its derivatives were dissolved in the aqueous phase (as in *Cell I*), the same evolution of the half-wave transfer potential with increasing pH were observed in the three cases. This is illustrated in *Fig. 2* for the measurements carried out within *Cell I* and in *Fig. 3* for those carried out within *Cell II*.

Comparison between piroxicam, *N*-Me-piroxicam, and *O*-Me-piroxicam reveals that the formal potential of transfer shifts by *ca.* 60 mV with each unit of pH (the slopes of the correlation lines vary between 49.5 mV and 60.7 mV with each unit of pH, due to experimental errors). This implies that the transfer becomes more and more difficult as the pH increases, since, according to *Eqn. 2*, the *Gibbs* transfer energy also rises with increasing pH.

Furthermore, the results of *Figs. 2* and *3* do not follow the transfer predicted and described above. Indeed, no transfer should be measured with piroxicam between pH 1.4 and 5.56 as well as with *N*-Me-piroxicam above pH 1.05, since both compounds are in their zwitterionic form in these pH ranges. Consequently, the measured half-wave potentials shown in *Figs. 3* and *4* cannot be due to piroxicam and its derivatives, but to proton transfer facilitated by piroxicam, *N*-Me-piroxicam, and *O*-Me-piroxicam, respectively.

Additionally, the experiments showed that the measured peak current was about two times higher with *Cell I* than with *Cell II*. Transfer was thus easier when piroxicam or one of its derivatives was first dissolved in the organic phase than when dissolved in the aqueous phase. Therefore, the measured transfer current suggests that the transfer

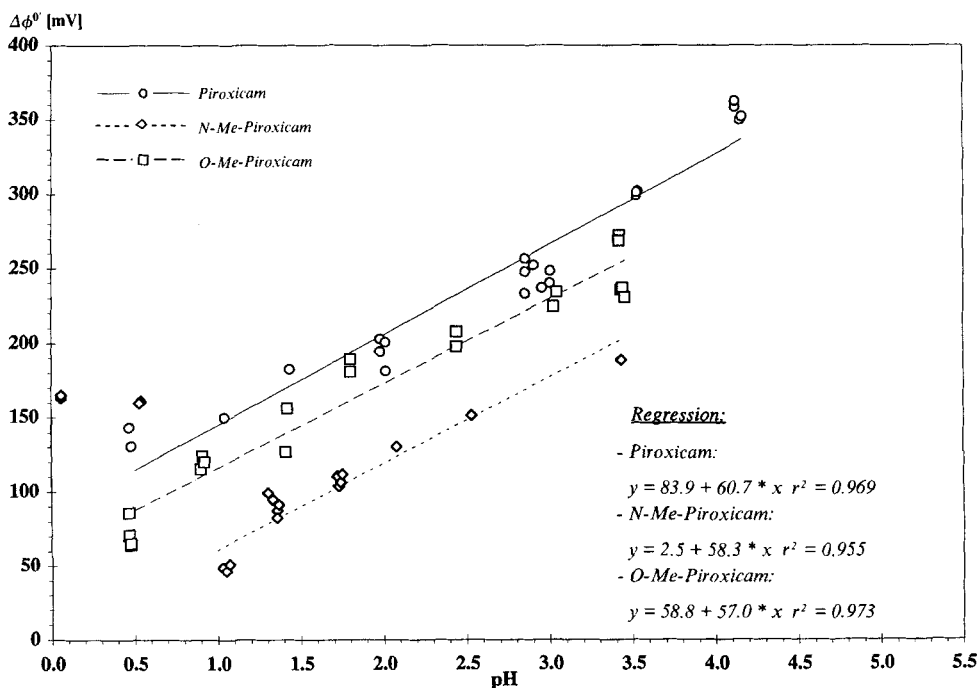


*Fig. 2.* Evolution of formal transfer potential with pH, when piroxicam, *N*-Me-piroxicam, and *O*-Me-piroxicam were dissolved in the aqueous phase (*Cell II*)

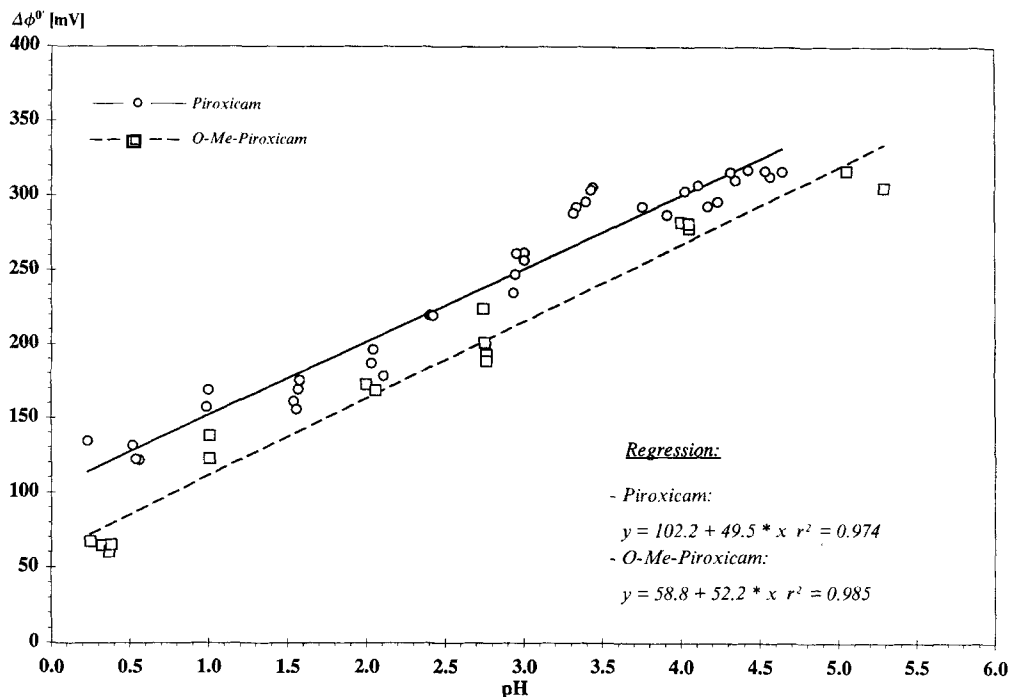
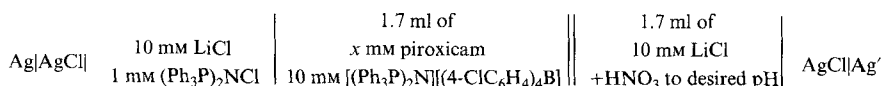


Fig. 3. Evolution of formal transfer potential with pH, when piroxicam and O-Me-piroxicam were dissolved in the organic phase (Cell II)

occurred by interfacial complexation/dissociation (TIC/TID) mechanism [51] (transfer by interfacial complexation/transfer by interfacial decomplexation). On the forward scan, the applied *Galvani* potential increased proton concentration at the interface where it transferred by a complexation reaction; on the reverse scan, the applied *Galvani* potential forced the complex to the interface where it dissociated releasing the proton. The piroxicam present in the organic phase thus plays the role of an ionophore and is protonated to allow transfer, as schematically described in Fig. 4.

**3.3. Piroxicam Concentration Profile.** To examine the possibility of an assisted proton transfer, the effect of piroxicam concentration on the peak current was studied. This experiment was carried out using *Cell III* at pH 1.0 and 3.6. The required amount of a 5 mM piroxicam + 10 mM [(Ph<sub>3</sub>P)<sub>2</sub>N][(4-ClC<sub>6</sub>H<sub>4</sub>)<sub>4</sub>B] solution was directly added to the organic phase to adjust the desired piroxicam concentration, and the transfer was then measured by cyclic voltammetry as a function of sweep rate.

#### Cell III



where  $x = 0, 0.03, 0.08, 0.18, 0.48, 0.71, 0.96, 1.45,$  and  $1.74$

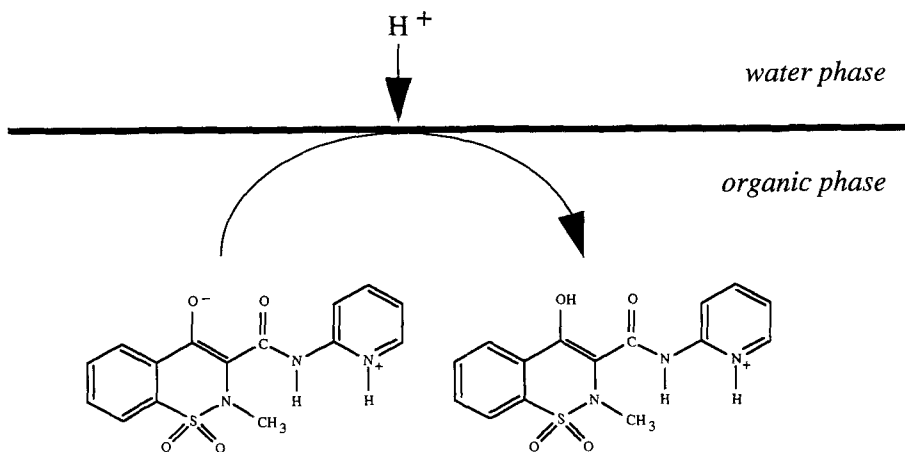


Fig. 4. Schematic description of the reaction mechanism for proton transfer assisted by piroxicam (transfer by interfacial complexation/decomplexation)

As the transfer is limited by diffusion to the interface, the plot of the peak current against the square root of the sweep rate should give a straight line [49]. Fig. 5 shows that the measured peak currents are in good agreement with the *Randles-Sevcik* plots represented for each piroxicam concentration when the aqueous pH is 1.0. Up to 1.74 mM piroxicam in  $\text{ClCH}_2\text{CHCl}_2$ , the peak currents vary linearly with the square root of the sweep rate, and the slopes of the respective regression lines increase with the piroxicam concentration.

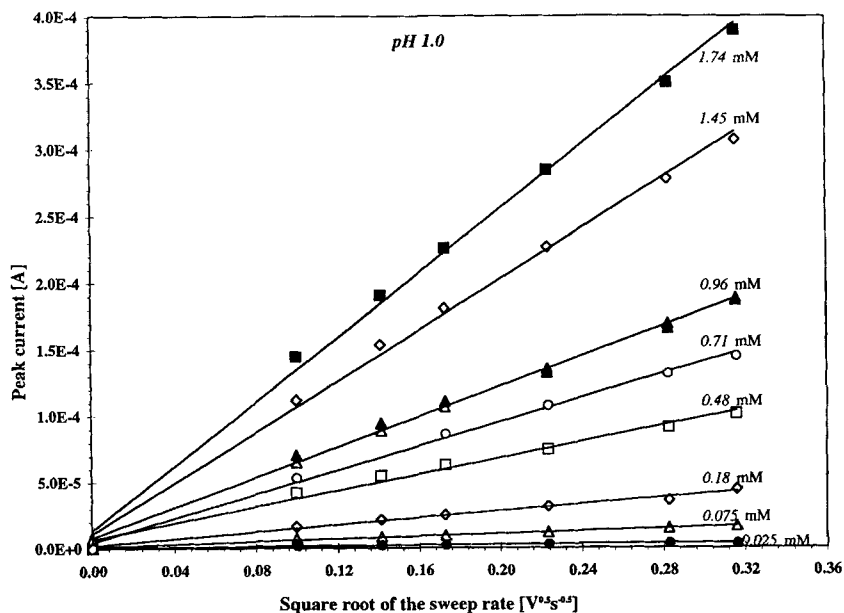
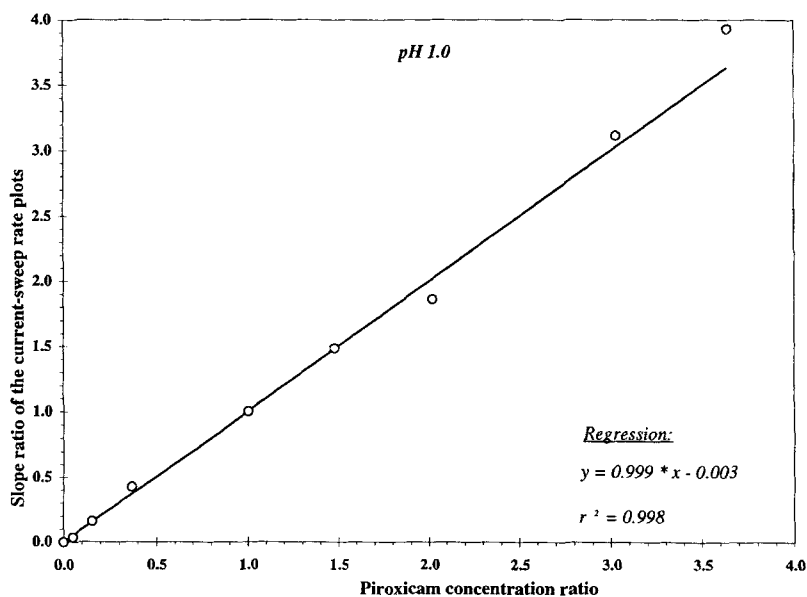


Fig. 5. Peak-current dependence on the square root of the sweep rate for different piroxicam concentrations in the organic phase

In fact, as the transfer current is proportional to the bulk concentration of the transferring species, the current ratio between two measurements at a given sweep rate should be equal to the concentration ratio between the same measurements. This is valid at any sweep rate and for all piroxicam concentration ratios. Therefore, the ratio of the slopes of the regression lines of the *Randles-Sevcik* plots allows a simplified interpretation of the results.

In the present case, the measurement at a piroxicam concentration of 0.48 mM gave a slope of  $3.08 \cdot 10^{-4} \text{ As}^{1/2} \text{ V}^{-1/2}$  and was taken as the reference. All the calculated slopes were then divided by that of the reference so as to obtain normalized ratios. In a similar manner, as the volumes of  $\text{H}_2\text{O}$  and  $\text{ClCH}_2\text{CH}_2\text{Cl}$  were both equal to 1.7 ml, the expected piroxicam concentration could be calculated for each addition. Piroxicam concentrations were then normalized with respect to that of 0.48 mM, in order to obtain a concentration ratio of 1 at this concentration. *Figs. 6* and *7* represent the evolution of the ratio of the slopes with the ratio of the piroxicam concentration when the aqueous pH was maintained at 1.0 or 3.6.

*Fig. 6* clearly shows that, at pH 1.0, the slope ratio of measured peak currents varied linearly with piroxicam concentration ratio ( $r^2 = 0.999$ ). This suggests that the amount of transferring species depends directly on piroxicam concentration, and that the transfer current was limited by the amount of piroxicam present in the organic phase.



*Fig. 6.* Ratio of the slopes of the regression lines of the *Randles-Sevcik* plots as a function of the ratio of piroxicam concentrations when the pH in aqueous phase was 1.0

*Fig. 7* shows that, at pH 3.6, the slope ratio of the regression line given by the *Randles-Sevcik* plots was equal to the piroxicam concentration ratio only when the latter ratio was  $< 1$ . When the ratio was  $> 1$ , the peak current did not change with increasing piroxicam concentration, and the calculated ratio of slopes remained constant. This

means that, at pH 3.6, the peak current was not limited by the concentration of piroxicam but by that of the proton. This suggests that piroxicam was not able to cross the interface and that the measured current was due entirely to the transfer of a proton from  $\text{H}_2\text{O}$  into  $\text{ClCH}_2\text{CH}_2\text{Cl}$  phase assisted by piroxicam.

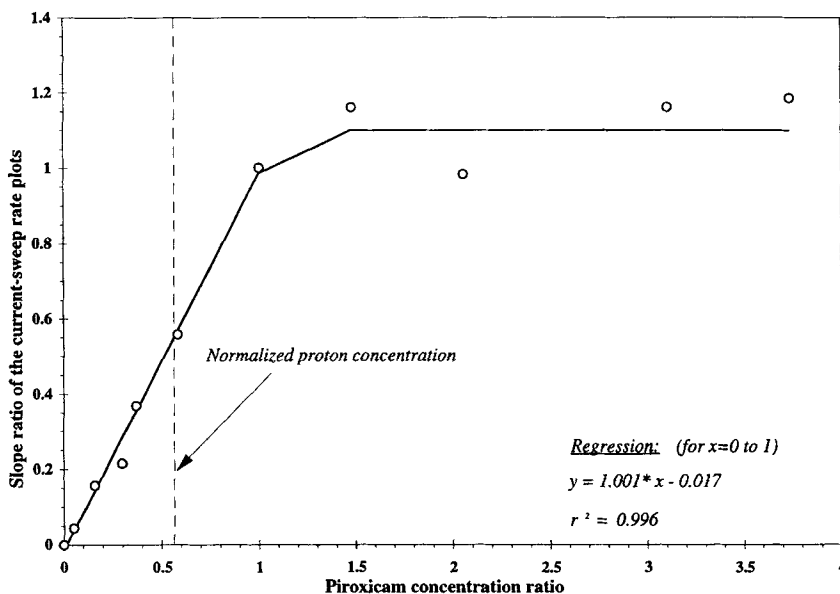


Fig. 7. Ratio of the slopes of the regression lines of the Randles-Sevcik plots as a function of the ratio of piroxicam concentrations when the pH in aqueous phase was 3.6

Indeed, if  $c_{\text{H}^+}^w \geq c_{\text{pi}}^o$ , the transfer is limited by the ionophore concentration and the measured transfer current increases proportionally with  $c_{\text{pi}}^o$ . On the other hand, if  $c_{\text{H}^+}^w \leq c_{\text{pi}}^o$ , the transfer is limited by proton concentration, and the current does not change with increasing ionophore concentration.

At pH 1.0, the proton concentration was equal to 0.1M, *i.e.*, *ca.* 60 times higher than the largest amount of piroxicam present in the organic phase during the experiments. Consequently, the proton was in very large excess and did not limit piroxicam transfer, as shown in Fig. 6.

However, the situation is more complex at pH 3.6. To simplify the discussion, we defined a normalized proton concentration at this pH by the ratio  $10^{-3.6} / (0.48 \cdot 10^{-3}) = 0.52$  (dotted line in Fig. 7). When the piroxicam concentration ratio was higher than the normalized proton concentration, piroxicam was in excess. Its transfer was then limited by proton concentration, and the peak current did not change with increasing piroxicam concentration. Here, the current still increased up to a piroxicam concentration ratio of 1 because of the difference in the diffusion coefficients of piroxicam and the proton.

Thus, both experiments confirm that the presence of piroxicam in the  $\text{H}_2\text{O}$  phase had no influence on the measured current, and that this current was due to a proton transfer assisted by piroxicam in the organic phase, as described in Fig. 4. This TIC/TID mecha-

nism was slightly different from the ‘usual’ facilitated transfer, as the proton transfer did not occur *via* a complexation reaction at the interface, but *via* a chemical reaction which transformed the neutral piroxicam into its protonated form.

3.4. *Dissociation Constants in the Organic Phase.* An important quantity which can be calculated from facilitated proton-transfer voltammograms as shown in *Fig. 1* is the dissociation constant in the organic phase,  $K_{\text{al}}^{\circ}$ , which, using the symbolism described in the *Scheme*, can be written for piroxicam as follows:

$$K_{\text{al}}^{\circ} = \frac{a_{\text{Pi}}^{\circ} a_{\text{H}^+}^{\circ}}{a_{\text{PiH}^+}^{\circ}} \quad (3)$$

If the proton concentration in  $\text{H}_2\text{O}$  phase is larger than that of the ligand in the organic phase, the dependence of the formal transfer potential of the protonated ionophore,  $\Delta_{\circ}^{\text{w}}\phi_{\text{LH}^+}^{\circ}$ , on the pH in  $\text{H}_2\text{O}$  phase can be determined by combining the *Nernst* equations at an ITIES [48] for both the proton and the protonated ionophore:

$$\Delta_{\circ}^{\text{w}}\phi_{\text{LH}^+}^{\circ} = \Delta_{\circ}^{\text{w}}\phi_{\text{H}^+}^{\circ} + \frac{RT}{2F} \ln\left(\frac{D_{\text{L}}^{\circ}}{D_{\text{LH}^+}^{\circ}}\right) - \frac{RT}{F} \ln\left(\frac{c_{\text{H}^+}^{\text{w}}}{K_{\text{al}}^{\circ}}\right) \quad (4)$$

where  $D_{\text{L}}^{\circ}$  and  $D_{\text{LH}^+}^{\circ}$  are the organic diffusion coefficients of the ligand and the complex, respectively, and  $F = N_{\text{A}} \cdot e$  where  $e$  is the charge of a proton.

The organic association constant can thus be calculated by varying the proton concentration in the aqueous phase, if it is assumed that  $D_{\text{L}}^{\circ} = D_{\text{LH}^+}^{\circ}$ . This is a reasonable assumption, since both the ionophore and ionophore-proton complex are similar in size. The difference between  $\Delta_{\circ}^{\text{w}}\phi_{\text{LH}^+}^{\circ}$  and  $\Delta_{\circ}^{\text{w}}\phi_{\text{H}^+}^{\circ}$  was plotted as a function of pH, as shown in *Figs. 8* and *9* for piroxicam and its derivatives. These plots give a straight line with a slope equal to  $(RT \ln 10)/F$  within experimental errors. The extrapolation to zero concentration then allowed the determination of  $K_{\text{al}}^{\circ}$ .

General theoretical equations for the dependence of the formal transfer potential of the ion-ionophore complex on the proton concentration in aqueous phase have been developed by *Matsuda et al.* [36]. In the previously mentioned case where  $c_{\text{H}^+}^{\text{w}} \geq c_{\text{L}}^{\circ}$ , this dependence is expressed in terms of a new function,  $F_{\text{A}}$ :

$$F_{\text{A}} = \exp\left[\frac{F}{RT}\left(\Delta_{\circ}^{\text{w}}\phi_{\text{PiH}^+}^{\circ} - \Delta_{\circ}^{\text{w}}\phi_{\text{H}^+}^{\circ}\right)\right] = \left(\frac{K_{\text{al}}^{\circ}}{\xi P_{\text{L}} K_{\text{al}}^{\text{w}}}\right) + \left(\frac{K_{\text{al}}^{\circ}(1 + \xi P_{\text{L}})}{\xi P_{\text{L}}}\right)\left(\frac{1}{c_{\text{H}^+}^{\text{w}}}\right) \quad (5)$$

where  $\xi = (D^{\circ}/D^{\text{w}})^{1/2}$ , the diffusion coefficient of the aqueous-phase species is equal to  $D^{\text{w}}$ , and that of the organic phase is equal to  $D^{\circ}$ .  $P_{\text{L}}$  is the partition coefficient of the ligand between the two phases:

$$P_{\text{L}} = \frac{c_{\text{L}}^{\circ}}{c_{\text{L}}^{\text{w}}} \quad (6)$$

Plots of the function  $F_{\text{A}}$  vs.  $1/c_{\text{H}^+}^{\text{w}}$  yield a straight line, which allows the determination of the association constants in both phases, if the value of  $P_{\text{L}}$  is known. The application of *Eqn. 5* constitutes an interesting method of determining dissociation constants of drugs in an organic phase. It has the advantage of being a direct evaluation of  $\text{p}K_{\text{a}}^{\circ}$ , since it does not require the knowledge of the activity coefficients of the species present in the organic phase.

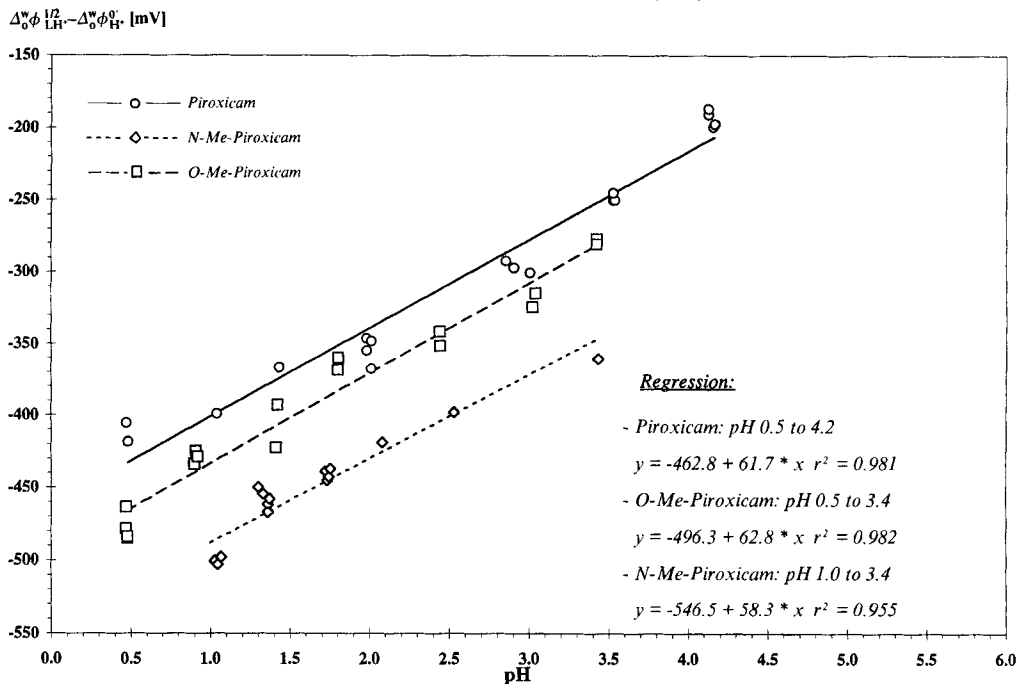


Fig. 8. Difference between the measured half-wave potential and the formal potential of the proton vs. pH: comparison between piroxicam and its derivatives dissolved in H<sub>2</sub>O

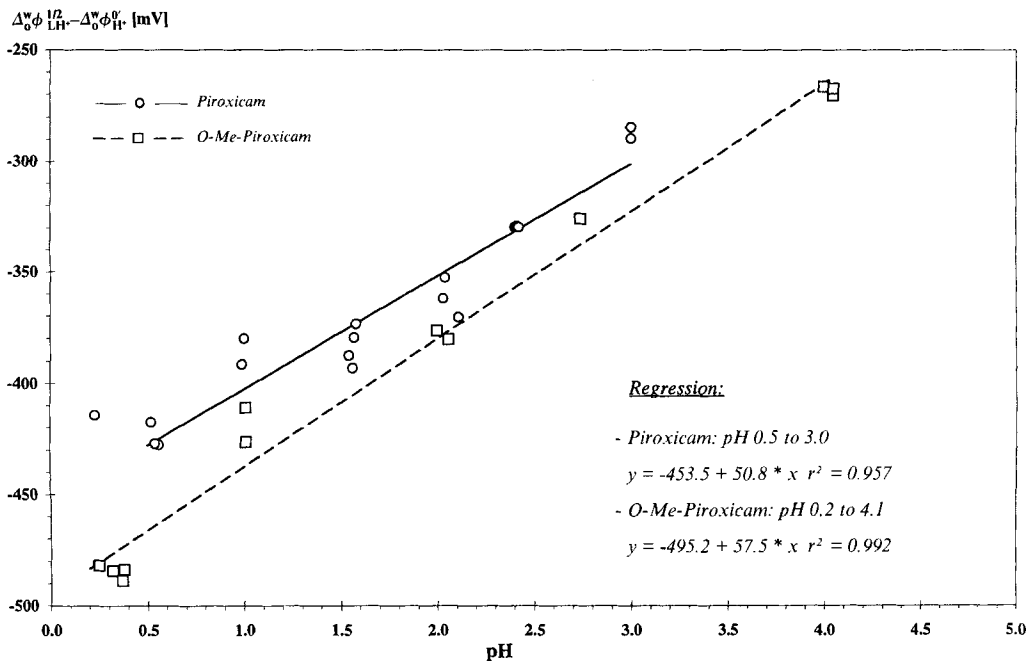


Fig. 9. Difference between the measured half-wave potential and the formal potential of the proton vs. pH: comparison between piroxicam and O-Me-piroxicam dissolved in C<sub>1</sub>H<sub>2</sub>CH<sub>2</sub>Cl

Values for  $F_A$  were calculated using Eqn. 5 for the experiments performed with Cells I and II, respectively, and were plotted against  $1/c_{H^+}^w$  as shown in Figs. 10 and 11. These plots yield a straight line with an intercept of zero within experimental errors. The resulting regression lines are also given in these figures for all experiments in order to check the accuracy of the analysis.

On the basis on Walden's rule [49],  $\xi$  was approximated to 1.12, and was then used with the values of  $P_L$  (see Table 1) to calculate the various  $pK_a^o$  values given in Table 2. Both Eqns. 4 and 5 were used for the calculation, so as to check the validity of the assumptions of the two models and their accuracy. The results are very close in both cases, which means that the diffusion coefficient of the ionophore in the organic phase is effectively equal to that of the complex.

These results show that the dissociation equilibria in the organic phase does not follow those in the  $H_2O$  phase: piroxicam has the lowest  $pK_a^o$  value and *N*-Me-piroxicam the highest, as proton activity is very small in  $ClCH_2CH_2Cl$ , the dissociation equilibria are constantly shifted toward the right, so as to favor the species of lower global charge. Tautomerism also explains how the zwitterionic forms of piroxicams can be stabilized by the intramolecular delocalization of their respective charges.

Moreover, the  $pK_a^o$  values are displaced by six to eight units with respect to their corresponding  $pK_a^w$  values. This means that the piroxicams have a smaller affinity for protons and, consequently, that they are less basic in  $ClCH_2CH_2Cl$  than in  $H_2O$ . This is due to the lack of H-bonds in  $ClCH_2CH_2Cl$ , which prevents the stabilization of a charge and favors the presence of neutral species.

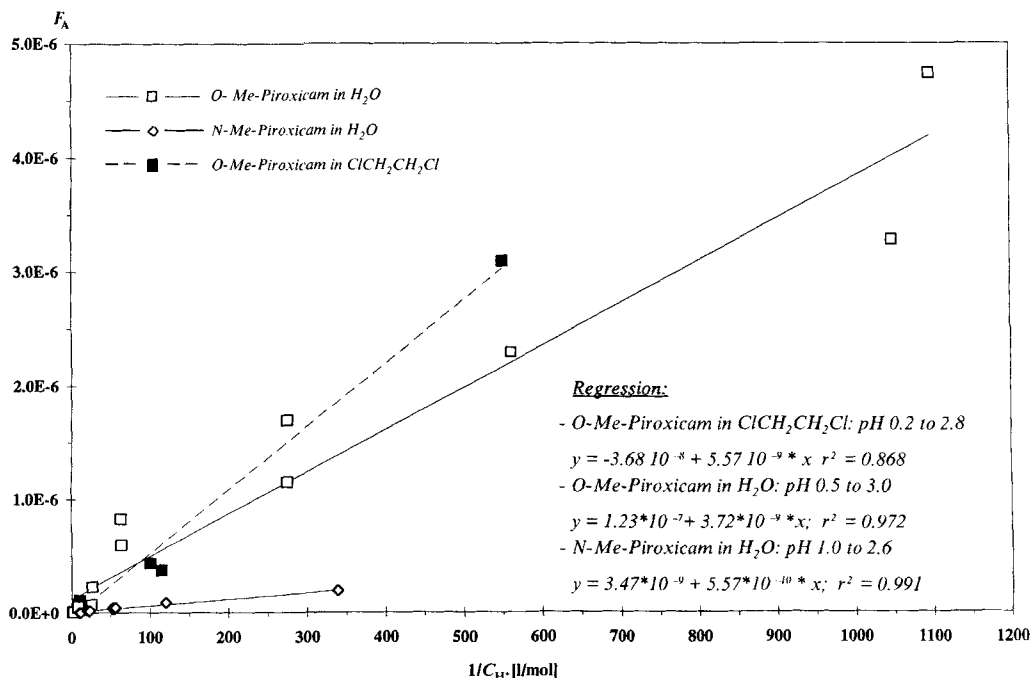


Fig. 10. Matsuda's function,  $F_A$ , vs.  $1/c_{H^+}^w$ : comparison between *O*-Me-piroxicam and *N*-Me-piroxicam dissolved either in  $H_2O$  or in  $ClCH_2CH_2Cl$

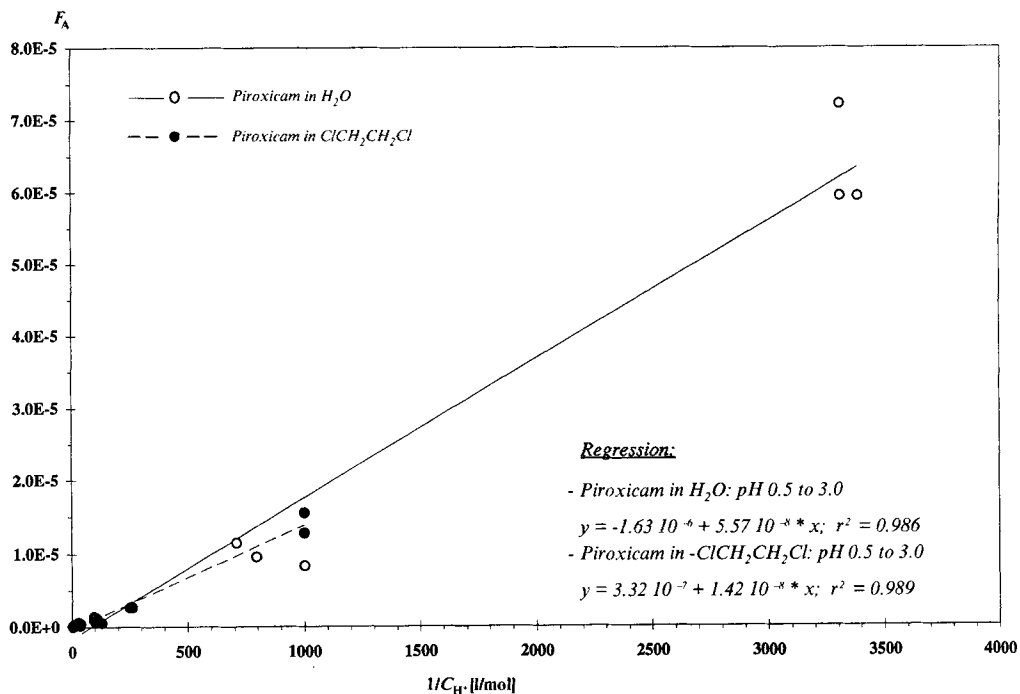


Fig. 11. Matsuda's function,  $F_A$ , vs.  $1/C_{H^+}$ : comparison between piroxicam dissolved in  $H_2O$  and piroxicam dissolved in  $ClCH_2CH_2Cl$

Table 2. Organic Dissociation Constants,  $pK_{a1}^o$ , of Piroxicam and Derivatives Calculated by Matsuda's Method

	Piroxicam <sup>a)</sup>	Piroxicam <sup>b)</sup>	<i>N</i> -Me-Piroxicam <sup>a)</sup>	<i>O</i> -Me-Piroxicam <sup>a)</sup>	<i>O</i> -Me-Piroxicam <sup>b)</sup>
$pK_{a1}^{o1)}$	$7.82 \pm 0.27$	$7.67 \pm 0.23$	$9.24 \pm 0.26$	$8.39 \pm 0.17$	$8.37 \pm 0.15$
$pK_{a1}^{o2)}$	$7.72 \pm 0.16$	$7.85 \pm 0.16$	$9.25 \pm 0.15$	$8.43 \pm 0.12$	$8.26 \pm 0.09$
Mean of $pK_{a1}^o$	$7.77 \pm 0.22$	$7.76 \pm 0.20$	$9.25 \pm 0.22$	$8.41 \pm 0.15$	$8.31 \pm 0.12$

<sup>1)</sup> Calculated with Eqn. 4.

<sup>2)</sup> Calculated with Eqn. 5.

<sup>a)</sup> Initially dissolved in  $H_2O$ .

<sup>b)</sup> Initially dissolved in  $ClCH_2CH_2Cl$ .

Furthermore, Table 2 clearly shows that the results obtained do not depend on the phase in which piroxicams were initially dissolved. The three compounds partition between the two phases on the time scale of the experiments, resulting in the same transfer behavior. This partitioning is then significant enough to allow a sufficiently large amount of the compounds to be present in the two phases and, consequently, to determine the  $pK_a^o$  values in both cases.

3.5. *Formal Gibbs Transfer Energy and Standard Distribution Coefficient.* The transfer of both proton and protonated compound ( $LH^+$ ) from the aqueous phase into the organic phase may occur, when an electrical-potential difference is applied across the interface,

which modifies the acid-base equilibrium in the vicinity of the interface. The distribution of the species in solution, therefore, depends on the protonation equilibrium and on the applied potential. Indeed, when  $(1 + \xi P_L) \gg c_{H^+}^w / K_{a1}^w$  in Eqn. 5, Matsuda's model describes the transfer of  $H^+$  assisted by the ionophore, since, when  $(1 + \xi P_L) \ll c_{H^+}^w / K_{a1}^w$ , the model represents the transfer of the ionized ionophore itself. In the latter case, the theory of simple ion transfer applies, and the transfer process in this region can be expressed by the thermodynamic cycle described in Fig. 12. It consists of a reaction layer on both sides of the interface and of the bulk phases acting as diffusion layers.

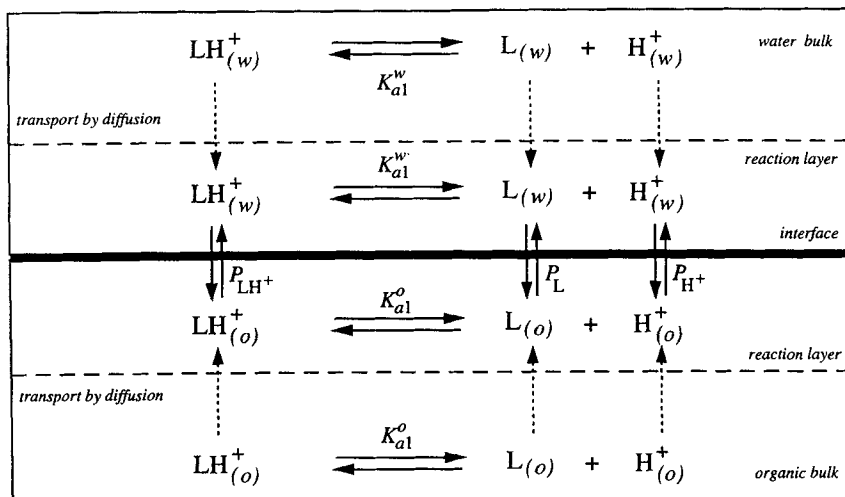


Fig. 12. Thermodynamic equilibria for the transfer of the various species present in the electrochemical cell

Following the description of Fig. 12, the formal transfer potential of the ionized ionophore is the only unknown parameter, since  $\Delta_{\circ}^w \phi_{H^+}^{\circ}$  has been measured to be 549 mV [52]. All the concentrations are bound together by the definition of the partition coefficient (Eqn. 6), that of the dissociation constants in both phases (Eqn. 3) and by the Nernst equations, and  $\Delta_{\circ}^w \phi_{LH^+}^{\circ}$  can thus be determined by solving this set of equations:

$$\Delta_{\circ}^w \phi_{LH^+}^{\circ} = \Delta_{\circ}^w \phi_{H^+}^{\circ} + \frac{RT \ln 10}{zF} (pK_{a1}^w - pK_{a1}^o - \log P_L) + \frac{RT}{zF} \ln \left( \frac{\gamma_{H^+}^{\circ} \gamma_{LH^+}^w}{\gamma_{H^+}^w \gamma_{LH^+}^{\circ}} \right) \quad (7)$$

where  $\gamma_i^w$  and  $\gamma_i^{\circ}$  are the activity coefficients of the species  $i$  in the aqueous and in the organic phase, respectively.

It should be stressed at this point that the expression of  $\Delta_{\circ}^w \phi_{LH^+}^{\circ}$  derived by Matsuda (Eqn. 5) gives the same results. Indeed, the formal transfer potential of  $LH^+$  itself is given by the value of  $\Delta_{\circ}^w \phi_{LH^+}^{\circ}$  when  $c_{H^+}^{w+tot}$  tends to infinity. This demonstrates that both methods describe effectively the same transfer mechanism, and thus that they are equivalent.

Knowing the formal transfer potential of the ionized form of piroxicam, its formal Gibbs transfer energy is then directly deduced from its definition (Eqn. 2):

$$\Delta G_{tr, LH^+}^{0,w \rightarrow o} = z_{LH^+} F \Delta_{\circ}^w \phi_{LH^+}^{\circ} = \mu_{LH^+}^{0,o} - \mu_{LH^+}^{0,w} + \frac{RT}{z_{LH^+} F} \ln \left( \frac{\gamma_{LH^+}^{\circ}}{\gamma_{LH^+}^w} \right) \quad (8)$$

Finally, the standard partition coefficients of the protonated ionophore  $P_{\text{LH}^+}^0$  (*i.e.*, the partition coefficient when the interface is not polarized [40]) follows directly from the *Nernst* equation:

$$\log P_{\text{LH}^+} = \log \left( \frac{c_{\text{LH}^+}^{\circ}}{c_{\text{LH}^+}^{\text{w}}} \right) = \frac{z_{\text{LH}^+} F}{RT \ln 10} (\Delta_{\circ}^{\text{w}} \phi - \Delta_{\circ}^{\text{w}} \phi_{\text{LH}^+}^{\circ}) = \frac{z_{\text{LH}^+} F \Delta_{\circ}^{\text{w}} \phi}{RT \ln 10} - \frac{\Delta G_{\text{tr,LH}^+}^{\circ, \text{w} \rightarrow \circ}}{RT \ln 10} \quad (9)$$

or

$$\log P_{\text{LH}^+} = \log P_{\text{LH}^+}^0 + \frac{z_{\text{LH}^+} F \Delta_{\circ}^{\text{w}} \phi}{RT \ln 10} \quad (10)$$

In first approximation, the term involving the ratio of the activity coefficients in *Eqns.* 7 and 8 can be neglected, so that the different parameters described above can be calculated. *Table 3* sums up the various results obtained for protonated piroxicam and its derivatives, when the mean value of  $\text{p}K_{\text{a}}^{\circ}$  is taken into account for the calculation.

Table 3. Formal Transfer Potential ( $\Delta_{\circ}^{\text{w}} \phi_{\text{LH}^+}^{\circ}$ ), Formal Gibbs Transfer Energy ( $\Delta G_{\text{tr,LH}^+}^{\circ, \text{w} \rightarrow \circ}$ ), and Standard  $\text{ClCH}_2\text{CH}_2\text{Cl}|\text{H}_2\text{O}$  Partition Coefficient ( $\log P_{\text{LH}^+}^0$ ) of Piroxicam, *O*-Me-Piroxicam, and *N*-Me-Piroxicam

	Piroxicam	<i>N</i> -Me-Piroxicam	<i>O</i> -Me-Piroxicam
$\Delta_{\circ}^{\text{w}} \phi_{\text{LH}^+}^{\circ}$	$16 \pm 2$	$-7 \pm 2$	$93 \pm 1$
$\Delta G_{\text{tr,LH}^+}^{\circ, \text{w} \rightarrow \circ}$	$1.6 \pm 0.2$	$-0.7 \pm 0.2$	$8.9 \pm 0.1$
$\log P_{\text{LH}^+}^0$	$-0.28 \pm 0.03$	$0.12 \pm 0.03$	$-1.57 \pm 0.02$

The results show that the energy necessary to transfer the protonated ionophores from aqueous into the organic phase is positive for  $\text{PiH}^+$  and *O*-Me $\text{PiH}^+$ , and negative for *N*-Me $\text{PiH}^+$  (see the *Scheme* for symbols). This suggests that *N*-Me $\text{PiH}^+$  is more stable in  $\text{ClCH}_2\text{CH}_2\text{Cl}$  than in  $\text{H}_2\text{O}$ , while the opposite applies for the two other compounds. Consequently, in their respective ionized forms,  $\text{PiH}^+$  and *O*-Me $\text{PiH}^+$  are less lipophilic than *N*-Me $\text{PiH}^+$ , which is confirmed by the values of the standard partition coefficients given in *Table 3*.

The lack of H-bonds in  $\text{ClCH}_2\text{CH}_2\text{Cl}$  prevents the stabilization of the protonated ionophores and favors the presence of the species of lower charge, so that  $\log P_{\text{L}}^0$  is more positive than  $\log P_{\text{LH}^+}^0$ , which is in good agreement with the results obtained.

In the case of *N*-Me-piroxicam, the charges of the zwitterion cannot delocalize due to the presence of the Me group. Thus, *N*-MePi is less lipophilic than Pi and *O*-MePi, which are globally neutral. Indeed, the proton in piroxicam may migrate toward the enolate group so as to neutralize the negatively charged O-atom. This intramolecular reaction allows piroxicam to be neutral and stabilizes it in  $\text{ClCH}_2\text{CH}_2\text{Cl}$ .

When piroxicam and its two derivatives are protonated, the situation is quite similar.  $\text{PiH}^+$  should be less lipophilic than *O*-Me $\text{PiH}^+$ , because a MeO group is more stable in  $\text{ClCH}_2\text{CH}_2\text{Cl}$  than a OH group. However, the charge on  $\text{PiH}^+$  can also delocalize by formation of intramolecular H-bonds. This prevents the formation of intermolecular H-bonds, and then diminishes the stabilization by the solvent. In this manner, the lipophilicity of  $\text{PiH}^+$  is increased. This stabilization effect is more important than that due to the presence of a MeO group, which explains why  $\log P_{\text{PiH}^+}^0$  is greater than  $\log P_{\text{O-MePiH}^+}^0$ .

Likewise, the values of  $\text{p}K_{\text{a}1}^{\circ}$  should be such that the species of lower charge is favored in the organic phase. Indeed, the larger  $\text{p}K_{\text{a}1}^{\circ}$  is big, the higher  $\text{LH}^+$  concentrations in order to satisfy the equilibrium. This is confirmed by the experimental results, since

*N*-Me-piroxicam is doubly charged in its *N*-MePi form and has the highest  $pK_{a1}^{\circ}$  value, while piroxicam has the lowest.

**4. Conclusion.** – The work presented here shows that piroxicam, *N*-Me-piroxicam and *O*-Me-piroxicam act so as to facilitate the transfer of protons at the interface between an aqueous and an organic phase. The results obtained demonstrate that the transfer follows an interfacial complexation/decomplexation mechanism, and that no direct ion transfer occurs. When the potential of the aqueous phase is rendered more positive with respect to that of the organic phase, the proton diffuses toward the interface and crosses it due to the protonation of the ionophore present in the organic phase. On the reverse scan however, the complex is forced to the interface where it dissociates releasing the proton into the aqueous phase. The pH dependence of the formal potential of transfer and the evolution of the transfer current with increasing concentrations of piroxicams confirm such a transfer mechanism.

The results obtained here show that cyclic voltammetry at the ITIES constitutes a suitable technique for the evaluation of thermodynamic parameters such as the formal potential of transfer and the dissociation constant of ionic drugs in an organic phase. For piroxicam and its two derivatives, it has been shown that they are less basic in  $\text{ClCH}_2\text{CH}_2\text{Cl}$  than in  $\text{H}_2\text{O}$ , since their  $pK_a^{\circ}$  values are shifted by *ca.* seven units with respect to their  $pK_a^w$  values. Unfortunately, it was not possible experimentally to determine the *Gibbs* transfer energy of the three protonated ionophores, due to their very low  $pK_a^w$  values, which resulted in perturbation of the measurements at very low values of pH and gave a very narrow potential window under such conditions. However,  $\Delta G_{tr,LH^+}^{o,w \rightarrow o}$  was calculated by resolution of the various thermodynamic equilibria describing the transfer. These values are in good agreement with the nature of the three ionophores and represent a first approximation of their partition between the two phases and of the energy needed to cross the interface.

The parameters determined here contribute to an improved understanding of the transfer mechanisms of piroxicam and more generally of the physicochemical mechanisms governing ionized drug transfer across lipidic membranes. Furthermore, access to membrane-bound enzymes and receptors also depends in part on ionic diffusion in lipidic environment. Such considerations are relevant to ionic drugs taken globally and may thus be of general interest.

This consideration applies to piroxicam specifically and, hypothetically, also to other anti-inflammatory agents. Indeed, inflammation is accompanied by pH lowering in affected tissues. Major inflammatory agent act by inhibiting cyclooxygenase and prostaglandin production, and by scavenging reactive oxygen species. Facilitated proton transfer, if it affects intracellular and tissular pH, could be seen as an additional mechanism to control inflammation. Modulation of intracellular pH has indeed been proposed as a novel therapeutic target [17].

*P.-A. C., H. G., and B. T.* are grateful for the financial support by the *Swiss National Science Foundation*.

#### REFERENCES

- [1] S. F. Timashev, 'Physical Chemistry of Membrane Processes', Ed. T. J. Kemp, Ellis Horwood, New York, 1991, pp. 15–246.
- [2] M. Bloom, E. Evans, O. G. Mouritsen, *Quarterly Rev. Biophys.* **1991**, *24*, 293.
- [3] M. A. Perillo, D. A. Garcia, A. Arce. *Mol. Membrane Biol.* **1995**, *12*, 217.

- [4] J. K. Seydel, E. A. Coats, H. P. Cordes, M. Wiese, *Arch. Pharm.* **1994**, 327, 601.
- [5] D. A. Smith, B. C. Jones, D. K. Walker, *Med. Res. Rev.* **1996**, 16, 243.
- [6] A. C. Chakrabarti, I. Clark-Lewis, P. R. Cullis, *Biochemistry* **1994**, 33, 8479.
- [7] G. M. Pauletti, H. Wunderli-Allenspach, *Eur. J. Pharm. Sci.* **1994**, 1, 273.
- [8] R. P. Austin, A. M. Davis, C. N. Manners, *J. Pharm. Sci.* **1995**, 84, 1180.
- [9] E. Depaula, S. Schreier, *Biochim. Biophys. Acta* **1995**, 1240, 25.
- [10] E. Nakashima, R. Matsushita, T. Ohshima, A. Tsuji, F. Ichimura, *Drug Metab. Dispos.* **1995**, 23, 1220.
- [11] L. Simchowicz, A. Roos, *J. Gen. Physiol.* **1985**, 85, 443.
- [12] M. F. Beal, B. T. Hyman, W. Koroshetz, *Trends Neurosci.* **1993**, 16, 125.
- [13] S. Simon, D. Roy, M. Schindler, *Proc. Natl. Acad. Sci. U.S.A.* **1993**, 91, 1128.
- [14] P. S. Treuhart, D. J. McCarty, *Arthritis Rheum.* **1971**, 14, 701.
- [15] R. I. Fox, H. I. Hang, *Lupus* **1993**, 2, S9.
- [16] L. Simchowicz, E. J. Crago, *Mol. Pharmacol.* **1986**, 30, 112.
- [17] P. McNiff, R. P. Robinson, C. A. Gabel, *Biochem. Pharmacol.* **1995**, 50, 1421.
- [18] Z. Samec, D. Homolka, V. Marecek, *J. Electroanal. Chem.* **1982**, 135, 265.
- [19] A. Sabela, J. Koryta, O. Valent, *J. Electroanal. Chem.* **1986**, 204, 267.
- [20] J. Koryta, *Selective Electrode Rev.* **1991**, 13, 133.
- [21] Y. Shao, H. H. Girault, *J. Electroanal. Chem.* **1992**, 334, 203.
- [22] E. Wang, Z. Yu, D. Qi, C. Xu, *Electroanalysis* **1993**, 5, 149.
- [23] Z. Yoshida, H. Aoyagi, Y. Meguro, Y. Kitatsuji, S. Kihara, *J. Alloys Compounds* **1994**, 213/214, 324.
- [24] M. D. Osborne, H. H. Girault, *Electroanalysis* **1995**, 7, 425.
- [25] E. Makrlík, W. Ruth, P. Vanysek, *J. Colloid. Interface Sci.* **1983**, 96, 548.
- [26] Y. N. Kozlov, J. Koryta, *Anal. Lett.* **1983**, B16, 255.
- [27] D. Homolka, V. Marecek, Z. Samec, K. Base, W. Wendt, *J. Electroanal. Chem.* **1984**, 163, 159.
- [28] Y. Shao, S. N. Tan, V. Devaud, H. H. Girault, *J. Chem. Soc., Faraday Trans.* **1993**, 89, 4307.
- [29] Z. M. Hu, W. Q. Zhang, P. S. Zhao, D. Y. Qi, *Electroanalysis* **1995**, 7, 681.
- [30] Y. Kudo, Y. Takeda, H. Matsuda, *J. Electroanal. Chem.* **1995**, 396, 333.
- [31] T. Ohkouchi, T. Kakutani, M. Senda, *Bioelectrochem. Bioenerg.* **1991**, 25, 81.
- [32] T. Ohkouchi, T. Kakutani, M. Senda, *Bioelectrochem. Bioenerg.* **1991**, 25, 71.
- [33] S. N. Tan, H. H. Girault, *J. Electroanal. Chem.* **1992**, 332, 101.
- [34] L. M. Yudi, A. M. Baruzzi, V. M. Solis, *J. Electroanal. Chem.* **1992**, 328, 153.
- [35] V. Marecek, Z. Samec, J. Koryta, *Adv. Colloid Interface Sci.* **1988**, 29, 1.
- [36] H. Matsuda, Y. Yamada, K. Kanamori, Y. Kudo, Y. Takeda, *Bull. Chem. Soc. Jpn.* **1991**, 64, 1497.
- [37] WHO, '1,2-Dichloroethane', in 'Environmental Health Criteria', 2nd edn., 1995, No. 176, pp. 1–148.
- [38] P. D. Hammen, H. Berke, J. Bordner, A. C. Braisted, J. G. Lombardino, E. B. Whipple, *J. Heterocycl. Chem.* **1989**, 26, 11.
- [39] K. Takacs-Novak, J. Kőkösi, B. Podanyi, B. Noszal, R.-S. Tsai, G. Lisa, P.-A. Carrupt, B. Testa, *Helv. Chim. Acta* **1995**, 78, 553.
- [40] F. Reymond, G. Steyaert, P.-A. Carrupt, B. Testa, H. H. Girault, *Helv. Chim. Acta* **1996**, 79, 101.
- [41] A. Avdeef, *J. Pharm. Sci.* **1993**, 82, 1.
- [42] N. El Tayar, R.-S. Tsai, P. Vallat, C. Altomare, B. Testa, *J. Chromatogr.* **1991**, 556, 181.
- [43] R.-S. Tsai, P.-A. Carrupt, B. Testa, 'Measurement of Partition Coefficients Using Centrifugal Partition Chromatography', in 'Modern Countercurrent Chromatography', Eds. W. D. Conway and R. J. Petroski, American Chemical Society, Washington, DC, 1995, Vol. 593, pp. 143–154.
- [44] G. Steyaert, G. Lisa, P.-A. Carrupt, B. Testa, F. Reymond, H. H. Girault, in preparation.
- [45] E. Bernhard, F. Zimmermann, *Arzneim.-Forsch.* **1984**, 34, 647.
- [46] R.-S. Tsai, P.-A. Carrupt, N. El Tayar, B. Testa, Y. Giroud, P. Andrade, F. Brée, J.-P. Tillement, *Helv. Chim. Acta* **1993**, 76, 842.
- [47] T. Wandlowski, V. Marecek, Z. Samec, *Electrochim. Acta* **1990**, 35, 1173.
- [48] H. H. Girault, 'Charge Transfer across Liquid/Liquid Interfaces', in 'Modern Aspects of Electrochemistry', Eds. J. O'M. Bockris, B. Conway, and R. White, Plenum Press, New York, 1993, Vol. 25, pp. 1–62.
- [49] A. J. Bard, L. R. Faulkner, 'Electrochemical Methods: Fundamentals and Applications', J. Wiley & Sons, New York, 1980, pp. 152–154.
- [50] D. Homolka, K. Holub, V. Marecek, *J. Electroanal. Chem.* **1982**, 138, 29.
- [51] Y. Shao, M. D. Osborne, H. H. Girault, *J. Electroanal. Chem.* **1991**, 318, 101.
- [52] A. Sabela, V. Marecek, Z. Samec, R. Fuoco, *Electrochim. Acta* **1992**, 37, 231.